Applied Acoustics 71 (2010) 731–738

Contents lists available at ScienceDirect

Applied Acoustics

journal homepage: www.elsevier.com/locate/apacoust

Effect of the open roof on low frequency acoustic propagation in street canyons

O. Richoux *, C. Ayrault, A. Pelat, S. Félix, B. Lihoreau

LAUM, CNRS, Université du Maine, Av. O. Messiaen, 72085 Le Mans, France

ARTICLE INFO

Article history:
Received 16 October 2008
Received in revised form 8 October 2009
Accepted 23 March 2010
Available online 27 April 2010

Keywords:
Urban acoustics
Street canyon
Finite Difference in Time Domain method
Scale model
Modal decomposition
Image sources

ABSTRACT

This paper presents an experimental, numerical and analytical study of the open roof effect on acoustic propagation along a 3D urban canyon. The experimental study is led by means of a street scale model. The numerical results are performed with a 2D-Finite Difference in Time Domain approach adapted to take into account the acoustic radiation losses due to the street open roof. An analytical model, based on the modal decomposition of the pressure field in the street width mixed with a 2D image sources model including the reflection by the open roof, is also presented. Results are given for several frequencies in the low frequency domain. The comparison of these approaches shows a quite good agreement until $f = 100$ Hz at full scale. For higher frequency, experimental results show that the leakage, due to the street open roof, is not anymore uniformly distributed on all modes of the street. The notion of leaky modes must be introduced to model the acoustic propagation in a street canyon.

1. Introduction

Urban acoustic researches are divided in three thematics: the sources characterization and identification, the acoustic propagation and the noise perception in an urban context. This work enters in the second thematic: its purpose is to describe the propagation of sound emitted by known sources in a street by taking into account its physical morphology, particularly the open roof effect.

To study acoustic propagation in an urban context, several approaches are available: energy based methods [1–4] based on the estimation of a quadratic quantity (energy density or acoustic intensity), numerical methods [5,6] to estimate acoustic pressure or velocity and modal approach [7–9] to calculate the pressure or velocity fields.

Energy based methods are largely used in urban acoustics but concern a limited frequency range: the image sources method [1,2,10–12], the ray tracing approach [13], the radiosity method [14–16] and finally statistical methods of particle transport [3,4,17] are generally used for middle and high frequencies. All these approaches propose to model the effect of the street open roof by a complete absorption of the waves.

The numerical methods, as Finite Element Method (FEM) or Boundary Element Method (BEM), are restricted for urban acoustics to low frequencies for 2D case or very low frequencies for 3D case [6,5] because of the large time cost due to the discretization.

The modal approach, where the geometrical characteristics of the street are explicitly taken into account in the model, is generally not used due to the complexity of the medium and to the difficulty to determine the modes of an open space like a street canyon. For example, Bullen and Fricke [7] have studied the acoustic propagation in a guide with infinite height or more recently, the modal approach was used to calculate the 2D field in a street section, the acoustic radiation conditions being described by an equivalent sources distribution at the interface between the street and the free space [18]. This method was then extended to the 3D case by a 2.5D equivalent sources method [8,9].

This review highlights more particularly that the open aperture of the street on the half free space, essential characteristic of the urban environment, is modeled by a complete absorption of the wave by energy based approaches for middle and high frequencies. For low frequencies, this assumption of complete absorption is not justified: Hornikx and Forssén propose a method to describe the radiation conditions on the open roof in a 2D geometry (in a section) [18] and recent works deal with the 3D urban acoustic problem [8,9,19]. However, these methods are quite complex and can be costly in numerical time. Moreover, the specific effect of the open roof for low frequencies was not studied in the literature.

The aim of this paper is to study the open roof effect in the acoustic propagation along a street canyon at low frequencies. For this, a reflection coefficient is introduced in a simple analytical model based on modal and image sources approaches. This coefficient is determined versus frequency by fitting the modeled pressure field with the experimental one obtained in a street scale model. In order to study only the open roof effect, street facades are chosen smooth and considered as perfectly reflecting. This work provides a first study of the open roof effect on the acoustic propagation in street canyon at low frequencies. It leads to a

* Corresponding author. Tel.: +33 2 43 83 36 67; fax: +33 2 43 83 35 20.
E-mail address: olivier.richoux@univ-lemans.fr (O. Richoux).

0003-682X/$ - see front matter © 2010 Published by Elsevier Ltd.
doi:10.1016/j.apacoust.2010.03.004

simple analytical model which allows the understanding of the involved physical phenomena. These analytical results are confirmed by a numerical study based on a 2D-FDTD method adapted to describe 3D geometrical dispersion and to take into account the reflection phenomena due to the ground and the open roof. This method gives a numerical method with a low computational cost for low frequencies.

Experimental results, obtained with a street scale model are described in Section 2. The analytical study, based on the modal decomposition of the field in the street width, mixed with an image sources model to determine the attenuation due to the street open roof, is presented in Section 3. The numerical study, made with a 2D-Finite Difference in Time Domain (FDTD) computation adapted to take into account the acoustic radiation losses by the street open roof is presented in Section 4. Finally, in Section 5, experimental, analytical and numerical results are compared for several frequencies providing the validity and the limits of these models.

2. Experimental study of the open roof effect on the acoustic propagation in a street canyon

2.1. Experimental set-up

2.1.1. Scale model of the street

A 1/25 scale model of 0.27 m height and 0.2 m width with 3 m length is carried out (Fig. 1) corresponding at full scale to a 6.75 m height, 5 m width and 75 m length street. This scale model is fully described in [20]. In this work, the ground (varnished concrete) and the facades (varnished wooden cubes) are smooth (all cubes are aligned) and considered as perfectly reflecting. The scale model is put in a semi-anechoïc room.

On one side, the source is enclosed (Fig. 1) in a flat rigid wall while an anechoïc termination is carried out on the other side (Fig. 2b). This anechoïc termination is made of melamine dihedron designed to obtain a cut-off frequency around 750 Hz. This allows to consider the scale model of 3 m length as semi-infinite for acoustic frequencies greater than 1 kHz.

2.1.2. Sound source

The acoustic source in the street is a loudspeaker enclosed in a rigid box opened on a guide with a square cross-section (0.05×0.05 m^2). Two sorts of aperture in the input rigid wall are used for the experimental studies: a 0.05×0.05 m^2 square cross-section aperture and a circular aperture with 0.01 m diameter (Fig. 2a). The square cross-section aperture simulates a plane source up to 3400 Hz and the circular source simulates a point source.

2.1.3. Data acquisition system and post-processing

The acoustic pressure is measured in the speaker box and in the street by means of two 1/4 in. pressure microphones (B&K 4938) connected to a preamplifier (B&K 2670) and a conditioning amplifier (B&K Nexus 2693). The preamplifier with the microphone is put vertically in the scale model to minimize the acoustic diffraction at high frequencies and for practical use during displacement. The excitation signal is sinusoïdal with a variable frequency f. A 3D robot allows to obtain horizontal maps of the acoustic pressure RMS value along the street. The step of spatial sampling is 0.01 m on the x-axis and y-axis. The acquisition of the acoustic pressure is performed using a sampling frequency $F_s = 20f$ (20 points per period) during a time length $T_a = N_s/F_s$, where $N_s = 2000$ (100 periods) is the samples number. The RMS value of the acoustic pressure is determined by means of a Matlab program using a least mean square method to determine the mean value, the amplitude and the phase of the signal.

2.2. Experimental results

In this work, the acoustic propagation along a street canyon is studied for low frequency case. The study of the pressure field in a horizontal plane along the street is made for the frequencies f = 1000, 1500, 2000, and 2500 Hz. These frequencies correspond to f = 40, 60, 80, and 100 Hz at full scale.

Fig. 3a shows the acoustic pressure map along the street for f = 1000 Hz, with a square source centered on $y_s = 0.175$ m and $z_s = 0.07$ m. The map is measured at the height z = 0.07 m (source plane). Firstly, the attenuation increases along the street. Secondly, the shape of the acoustic map shows the presence of acoustic modes in the (x, y) plane of the street.

Fig. 3b shows acoustic pressure map along the street in the same geometrical configuration for f = 1500 Hz. The same remarks as for f = 1000 Hz can be made, except that the shape of the pressure map is not the same due to a different repartition of the source condition on the modes. We can note that the attenuation along the street is greater for f = 1500 Hz than for f = 1000 Hz. This

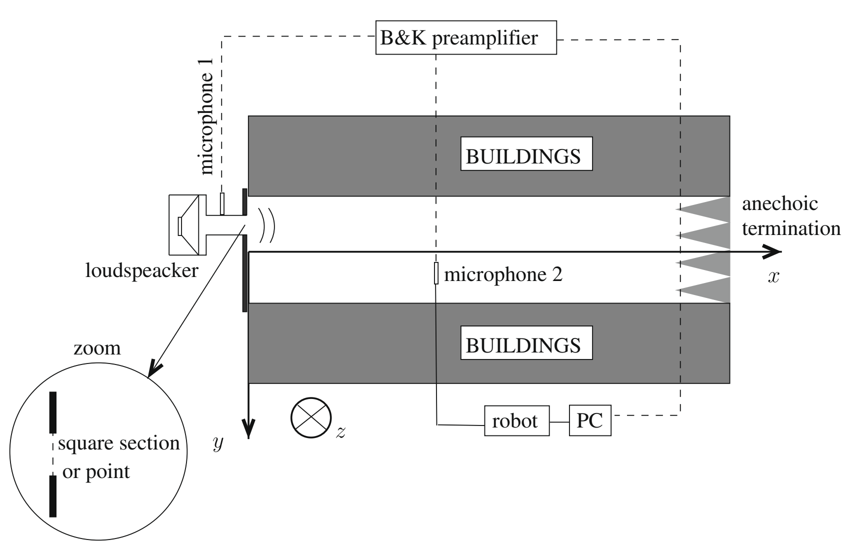

Fig. 1. Scheme of the experimental apparatus.

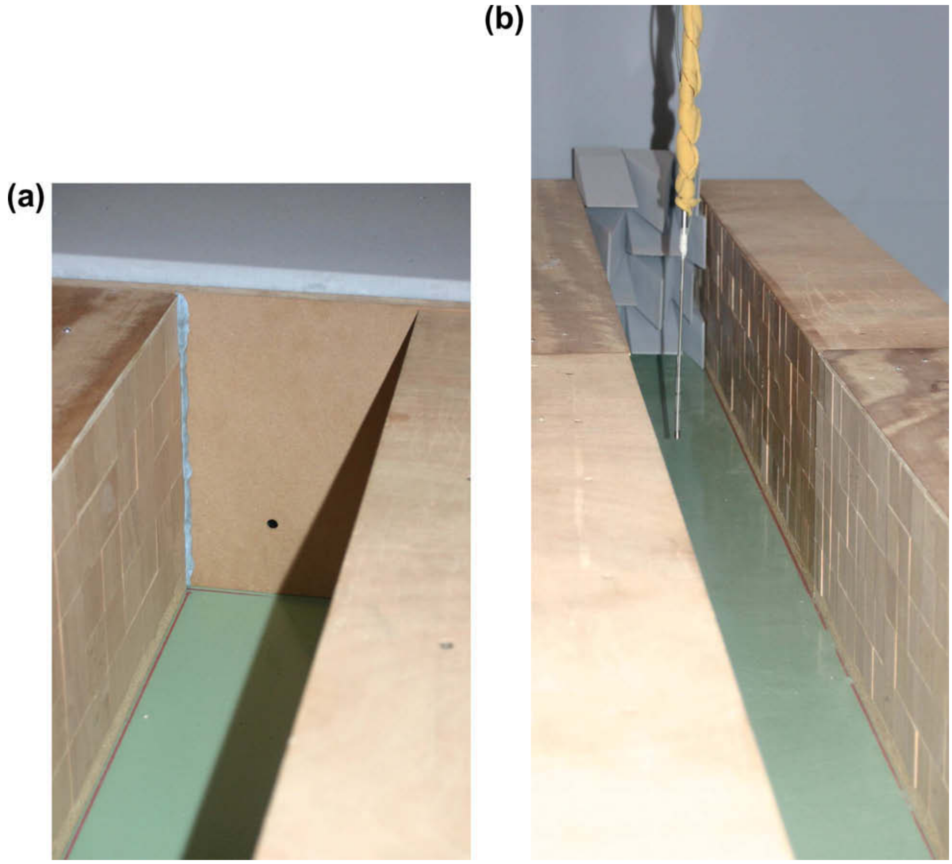

Fig. 2. Views of the street scale model. (a) Rigid wall with a circular aperture at the input. (b) anechoïc end.

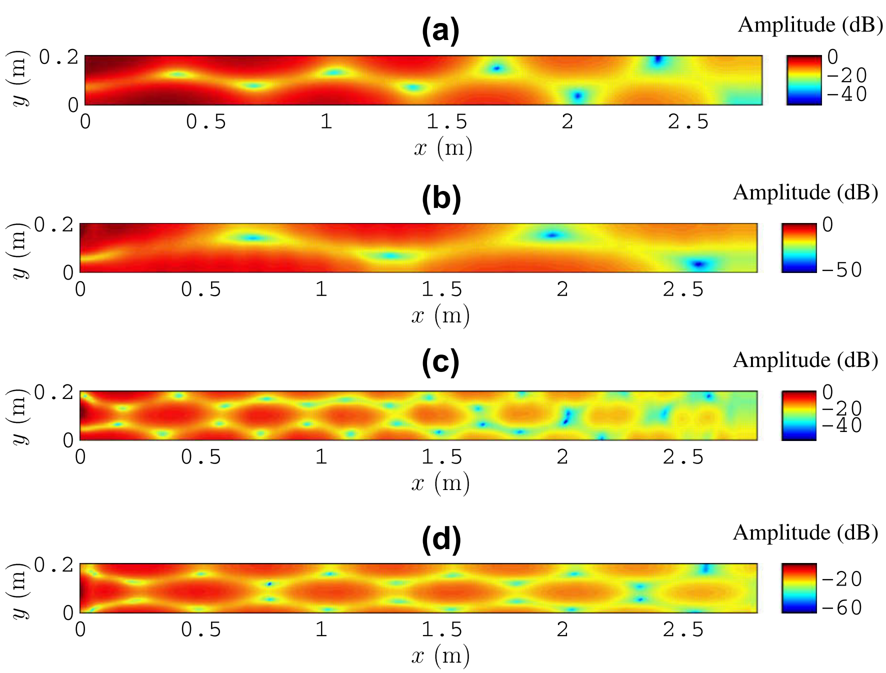

Fig. 3. Acoustic pressure in the street (scale model) for (a) $f = 1000$ Hz at $z = 0.07$ m and for a square source centered on ($y_s = 0.175$ m, $z_s = 0.07$ m), (b) $f = 1500$ Hz at $z = 0.07$ m and for a square source centered on ($y_s = 0.175$ m, $z_s = 0.07$ m), (c) $f = 2000$ Hz at $z = 0.07$ m and for a point source centered on ($y_s = 0.115$ m, $z_s = 0.07$ m), (d) $f = 2500$ Hz at $z = 0.07$ m and for a square source centered on ($y_s = 0.1$ m, $z_s = 0.07$ m).

attenuation increase shows that the acoustic losses due to the open roof depend on frequency.

Fig. 3c and d show the acoustic pressure map along the street for respectively $f = 2000$ Hz and $f = 2500$ Hz at $z = 0.07$ m. In these cases, a point source centered on $(z_s = 0.07\ \text{m},\ y_s = 0.115\ \text{m})$ for $f = 2000$ Hz and $(z_s = 0.07\ \text{m},\ y_s = 0.1\ \text{m})$ for $f = 2500$ Hz is used. The modal repartition of the source condition and the number of the propagative modes differ from the two previous cases (three modes are propagative). The attenuation along the street increases also with frequency.

These observations show that the open roof of the street brings acoustic losses for the pressure field inside the street. This attenuation is studied more precisely in the following section. In one hand, all these experimental maps show that the pressure on the (x, y) plane can be easily modeled by a modal decomposition of the field. On the second hand, for all cases, it appears that the attenuation increases along the street. This attenuation may be due to the roof, ground and facades absorption, and to atmospheric attenuation. However, at the studied frequencies (1000 Hz < f < 2500 Hz), atmospheric attenuation in the scale model (a few meters length) is negligible and ground and facades are assumed to be perfectly reflecting (the absorption coefficient in diffuse field of varnished concrete and wood is around 3% at 1000 Hz).

These considerations show that the acoustic attenuation is mainly due to the open roof of the street. Moreover, it appears that this attenuation increases with frequency. In regards to experimental conclusions, two models (analytical and numerical) of the acoustic propagation along a street are presented in the following sections to take into account this open roof absorption.

3. Analytical modelling of the open roof effect on acoustic propagation along a street

The analytical model of the acoustic propagation along a street is based on the modal decomposition of the pressure field in the transverse direction y (Fig. 4b). The attenuation of the pressure along the street, due to acoustic radiation losses through the open roof is described by means of a 2D image sources model in the vertical plane (x, z) (Fig. 4c). The combination of these two approaches allows to elaborate a 3D analytical model of the acoustic propagation along a street.

A semi-infinite 3D waveguide of width d closed by a rigid wall at $x = 0$ containing an acoustic source is considered (Fig. 4).

In spherical polar co-ordinate (r, θ, y) as shown in Fig. 4 and in the frequency domain (with a temporal convention $e^{j\omega t}$, where ω is the acoustic pulsation), the acoustic pressure $p(r, \theta, y)$ satisfies the Helmholtz equation [7]

$$\frac{\partial^2 p}{\partial r^2} + \frac{1}{r}\frac{\partial p}{\partial r} + \frac{\partial^2 p}{\partial y^2} + k^2 p = 0, \tag{1}$$

where $k = \omega/c$ with c the sound celerity. The solution of the Eq. (1) can be written as

$$p(r, \theta, y) = p(r, \theta)p(y). \tag{2}$$

The transversal solution $p(y)$ is given by

$$p(y) = \sum_{n=1}^{N} A_n \sqrt{2 - \delta_{n0}} \cos\left(\frac{n\pi}{d} y\right), \tag{3}$$

where δ_{n0} is the Kronecker symbol ($\delta_{n0} = \delta(n) = 1$ for $n = 0$ and $\delta_{n0} = 0\ \forall n \neq 0$) and N is the number of modes. To determine the amplitude A_n of each mode, the boundary condition given by the acoustic source is used.

To model the attenuation of the pressure field due to acoustic radiation losses through the street open roof, a 2D image sources model is used in the vertical plane (x, z) (Fig. 4c). In this plane, the ground of the street is considered as perfectly rigid with a reflection coefficient $R_g = 1$ and the source is described by a point source located at the height h_s embedded in a rigid wall with height h. The acoustic radiation condition corresponding to the open roof of the street is modeled by means of a reflection coefficient R_r at the height h on the z-axis.

The pressure field in the street can be decomposed as an infinite sum describing the multiple reflections on the ground and the street roof. In a 2D domain, the Green function $G(\vec{r}, \vec{r}_0)$ is written as

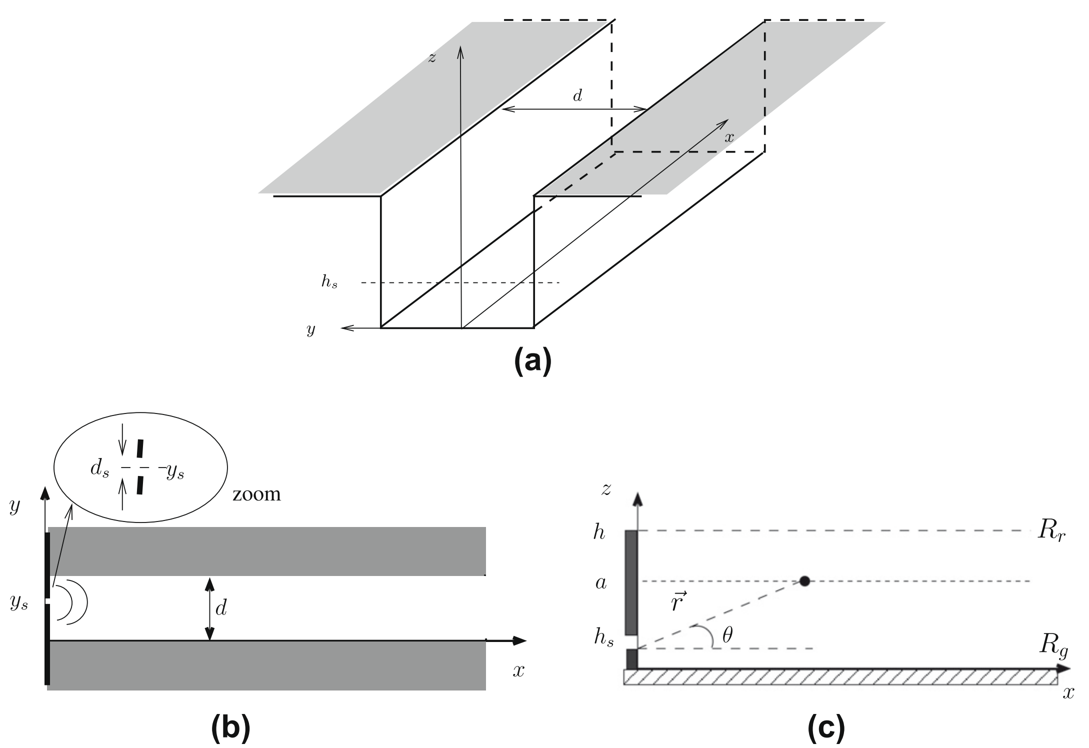

Fig. 4. View of the street (a) in the (x, y) plane (b) and in the (x, z) plane (c).

$$G(\vec{r},\vec{r}_0) = -\frac{j}{4}\left(H_0^1(k|\vec{r}-\vec{r}_0|)\right), \tag{4}$$

where $\vec{r}_0$ defines the position of the source and H_0^1 is the Hankel function of first order. According to Eq. (4), the pressure field of the mode n, at the altitude z in the street, takes the following form:

$$p_n(r,\theta) = -\frac{j}{4}\sum_{m=0}^{+\infty}(R_r)^m\left(H_0^1(k_{nr}|\vec{r}-\vec{r}_{0m}^{+}|) + H_0^1(k_{nr}|\vec{r}-\vec{r}_{0m}^{-}|)\right), \tag{5}$$

with $k_{nr}^2 = k^2 - (\frac{n\pi}{d})^2$ and $|\vec{r}-\vec{r}_{0m}^{\pm}| = \sqrt{x^2 + (z \pm 2mh \pm h_s)^2}$, where m corresponds to the m^{th} image source.

Finally, the pressure field $p(r,\theta,y)$ along the street taking into account the acoustic radiation losses due to the open roof is given by the following equation:

$$p(r,\theta,y) = -\frac{j}{4}\sum_n\left\{A_n\sqrt{2-\delta_{n0}}\cos\left(\frac{n\pi}{d}y\right)\sum_m(R_r)^m\left(H_0^1\left(k_{nr}|\vec{r}-\vec{r}_{0m}^{+}|\right) + H_0^1\left(k_{nr}|\vec{r}-\vec{r}_{0m}^{-}|\right)\right)\right\}. \tag{6}$$

In this problem, the experimental source is a square plane source or a point source. In the analytical model, the square source is described by a hole with a width d_s in a rigid wall on the street input along the direction y given by

$$v(y) = 1, \quad \text{for } y_s - d_s/2 < y < y_s + d_s/2, \tag{7}$$

$$v(y) = 0, \quad \text{for } 0 < y \leqslant y_s - d_s/2 \quad \text{and} \quad y_s + d_s/2 \leqslant y < d. \tag{8}$$

The source width along the z dimension can not be taken into account in the image sources model. This assumption is valid far from the source. On the other hand, the point source is well described in this model when d_s tends to 0.

In this work, the reflection coefficient R_r describing acoustic radiation leakage due to the street open roof is determined by fitting the model with the experimental results obtained in the street scale model.

4. Numerical simulation of the open roof effect on acoustic propagation along a street

To take into account the open roof effect on the acoustic propagation along a street, the 3D numerical methods are well suited. However, even at low frequencies, these methods have a high computation cost. Thus, in this work, we propose to model the open roof effect in a 2D-FDTD method which gives a simple and a low computational cost numerical method. This 2D-FDTD method has to describe the 3D geometrical dispersion and takes into account the reflection phenomena due to the ground and the open roof in order to be compared to experimental data in the street scale model.

In a 2D description, the geometrical dispersion is lower (decrease with $1/\sqrt{r}$ from the source) than in a 3D description (decrease with $1/r$ from the source). Thus, it is necessary to add a loss term in a 2D description to describe a 3D geometrical dispersion. Moreover, the losses due to the ground and roof absorption have to be modeled. In this 2D model, all the losses are introduced by means of a single negative source term $q(t)$ in the mass conservation law, leading to the following form:

$$\frac{dp(t)}{dt} + c^2\rho_0\vec{\nabla}\cdot\vec{v}(t) = \rho_0 c^2 q(t). \tag{9}$$

This negative source, uniformly distributed in the 2D plane, can be considered as proportional with the pressure $p(t)$ written as

$$q(t) = -\alpha p(t), \tag{10}$$

where $\alpha > 0$ is a coefficient to be determined.

The discrete forms of the Eqs. (9) and (10) and the Euler equation can be achieved by a two dimensional Finite Difference Time Domain (FDTD) computation. After the integration of the mass conservation along a surface element of dimension dx along the x-axis and dy along the y-axis, we obtain

$$\frac{dp}{dt}(x,y) + c^2\rho_0\left(\frac{dv_x}{dx}(x,y) + \frac{dv_y}{dy}(x,y)\right) = -\rho_0 c^2\alpha p(x,y), \tag{11}$$

where v_x and v_y are respectively the projections of the acoustic velocity along the x- and y-axis. The same approach is used with the Euler equation. The discretization of these two equations is achieved with a first order centered finite difference scheme with staggered spatial and temporal grids [21]. This allows to obtain a 2D-FDTD computation of the propagation in a 3D space.

To apply the adapted 2D-FDTD simulation to the propagation along a street with an open roof, the discrete equations are computed by means of a Matlab program where the boundary conditions are introduced on the acoustic velocity (the facades of the street are considered as perfectly rigid) and the source condition is introduced on the pressure. The anechoïc termination is simulated by a Perfect Matching Layers (PML). The coefficient α in the Eq. (11) is determined by fitting the simulation results with the experimental ones obtained in the street scale model.

5. Results and discussion

5.1. General observations

In this section, we propose a qualitative comparison between the experimental, analytical and numerical results for f = 1000 Hz, f = 1500 Hz and f = 2500 Hz. Fig. 5 presents results obtained at f = 1000 Hz, z = 0.07 m, for a square source centered on ($y_s = 0.175$ m, $z_s = 0.07$ m). The analytical results are computed by means of Eq. (6) with N = 56, m = 3 and $R_r = -0.3$. The reflection coefficient of the open roof is determined by fitting qualitatively the analytical and experimental pressure maps and more precisely on pressure lines over the x-axis, by fitting the pressure maxima magnitudes and positions. The numerical results are obtained with $\alpha = 1.8 \times 10^{-3}$ s^{-1} and with a spatial sampling of 0.01 m which provides 34 points per wavelength.

The qualitative agreement between simulated (analytical and numerical) and experimental results is correct: the shapes of the field are close and attenuations along the street are qualitatively of the same magnitude order, around 20 dB along 2.8 m. Since the ground and facades have a very small absorption coefficient (leading to a few dB attenuation along 2.8 m), this strong attenuation is necessarily mainly due to the open roof. In the analytical model, a reflection coefficient R_r is defined to describe the attenuation due to the open roof. This coefficient, in the order of -0.3, points out the role of the open roof which constitutes a impedance mismatch involving a reflected wave. As expected, this coefficient is negative, due to the open geometry of the street.

Secondly, from the middle of the street in the x direction, the location on the y-axis of the pressure nods of the experimental and numerical maps are shifted. These nods are confined progressively near the facades. Thus, the modal structure of the pressure field, defined in the first half part of the street, is progressively modified when x is increased. This is probably due to the facades absorption. In this case, the analytical model (with rigid facade assumption), cannot well describe the structure of the pressure field, in particular the pressure nods positions. On the contrary, numerical simulations, which take into account all losses in one absorption coefficient can describe this phenomenon. It appears also a slight shift of the pressure nods positions in the y direction between experimental and numerical results. This can be ex-

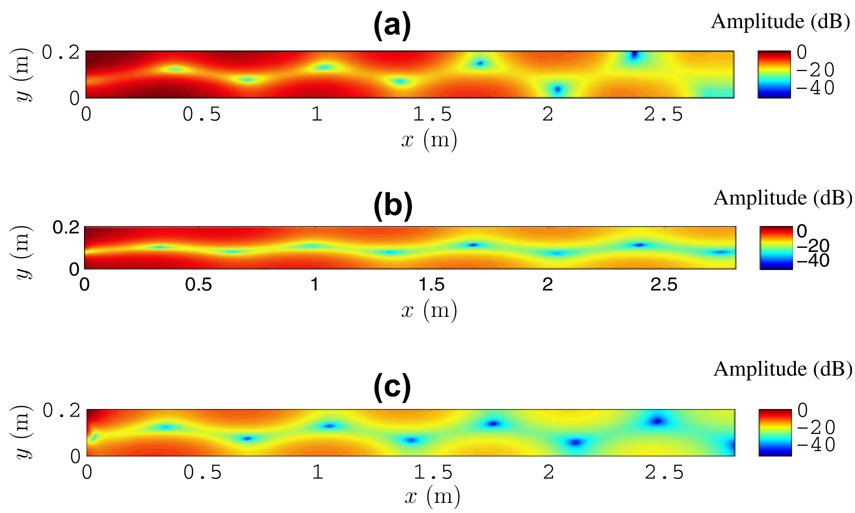

Fig. 5. Normalised acoustic pressure level for f = 1000 Hz at z = 0.07 m with a square source centered on ($y_s = 0.175$ m, $z_s = 0.07$ m): (a) experiments, (b) analytical model, (c) adaptated 2D-FDTD simulation.

plained by a default in the robot alignment in the y direction along the street x-axis which leads to a deviation between the experimental and simulated spatial grids. Finally, the slight shift of the pressure nods positions along the street (in the x direction) is due to this alignment default and to the choice of the loss term α provided by the fitting.

Such comparisons have been made for different frequencies and lead to the same qualitative conclusions. They show also a frequency dependance of R_r and α, describing the open roof effect. Next section presents more precisely this dependance.

5.2. Frequency dependence of the open roof effect

To study with more precision the differences between the experimental, analytical and numerical results and the frequency dependence of the open roof effect, the acoustic pressure is shown along the x-axis of the street with fixed y for different frequencies in the range (1000–2500) Hz. The analytical and numerical results are fitted to the experimental data by means of the maxima position and amplitude.

Fig. 6a and b present results for f = 1000 Hz at respectively y = 0.09 m and y = 0.15 m. The fitting is good for the pressure maxima amplitudes (deviation in order of 1 dB) and positions (estimation with maximum error of 0.05 m). Similarly, the node positions are quite well predicted. However, a great divergence (highlighted by the log representation) of the minima amplitudes estimation appears. This is due to the shifting of the different spatial grids (experimental, analytical and numerical) caused by the misalignment of the 3D robot.

At the street input, a deviation between the experimental and numerical results appears; the use of a 2D model cannot describe a 3D acoustic source conditions. On the contrary, the analytical model gives a good prediction of the near field due to its 3D geometry.

Similar experiments realized for a frequency of 1500 Hz provide the same results and conclusions with five image sources, $R_r = -0.1$, N = 59 for the analytical model and $\alpha = 1.9 \times 10^{-3}$ s^{-1} for the numerical one.

For f = 2000 Hz, the analytical, simulated and experimental results are compared on Fig. 7 for y = 0.08 m. The analytical model

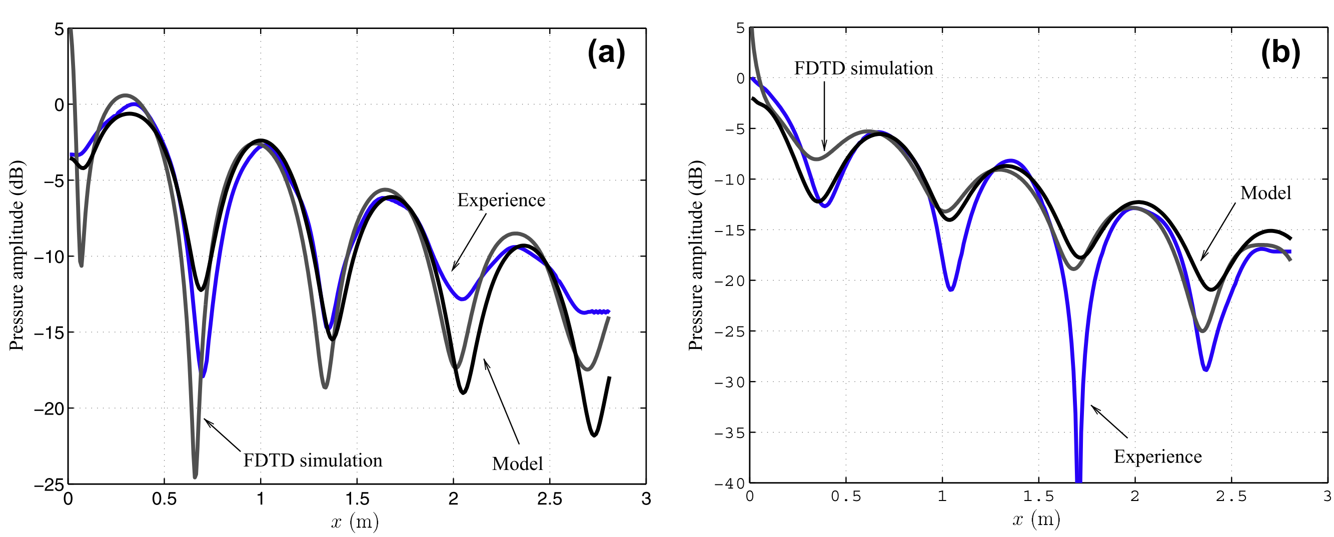

Fig. 6. Comparison of the experimental (blue curve), analytical (black curve) and numerical (gray curve) results of the pressure profile along the street for f = 1000 Hz (see Fig. 3 for geometrical configuration) at y = 0.09 m (a) and y = 0.15 m (b). (For interpretation of the references to colour in this figure legend, the reader is referred to the web version of this article.)

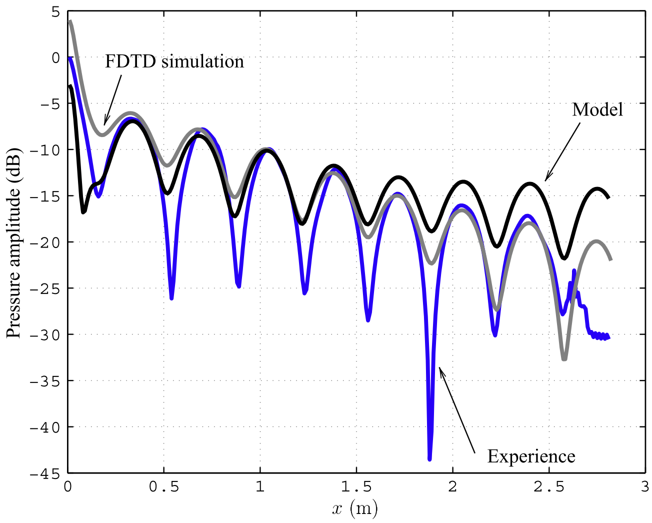

Fig. 7. Comparison of the experimental (blue curve), analytical (black curve) and numerical (gray curve) results for the pressure profile along the street for $f = 2000$ Hz (see Fig. 3 for geometrical configuration) at $y = 0.08$ m. (For interpretation of the references to colour in this figure legend, the reader is referred to the web version of this article.)

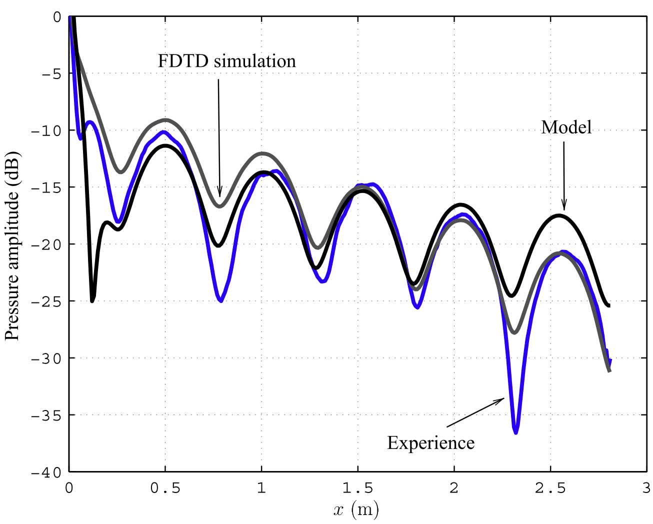

Fig. 8. Comparison of the experimental (blue curve), analytical (black curve) and numerical (gray curve) results of the pressure profile along the street for $f = 2500$ Hz (see Fig. 3 for geometrical configuration) at $y = 0.1$ m. (For interpretation of the references to colour in this figure legend, the reader is referred to the web version of this article.)

Table 1
Reflection coefficient R_r (analytical model) and absorption coefficient α (numerical model) versus frequency.

f (Hz)	1000	1500	2000	2500
α (10^{-3} s^{-1})	1.8	1.9	2	2.5
R_r	−0.3	−0.1	0	0

is computed with $R_r = 0$ and $N = 62$ and the simulated one is performed with $\alpha = 2 \times 10^{-3}$ s^{-1}.

The agreement between the numerical and experimental results is good: except for the near field (30 cm from the source), the attenuation is very well predicted and a error of 0.03 m on the maxima positions along the x-axis, involved by the shift of the spatial grid, is visible. In the near field, the acoustical path difference is in the order of the wavelength λ: the first experimental node at 0.15 m corresponds to a path difference of $\lambda/2$ between direct and reflected (by the ground) waves. These interferences cannot be described by a 2D model.

For the analytical results, the maxima positions are well estimated. The amplitude of the first maxima are well predicted until $x = 1.5$ m. In the near field, the reflexion on the ground is predicted with a weak deviation due to the definition of the source-receiver distance (Eq. (5)) in the (x, z) plane. Farther, this model underestimates the attenuation: this is probably due to the weak absorption of the facades (varnished wood) which modifies the experimental pressure field structure but which is not taken into account in the model. The misalignment of the robot leading to the shift of spatial grids (notably visible on Fig. 3c) may also contribute to this divergence.

Fig. 8 shows the experimental, analytical and simulated acoustic pressure along the x-axis for $f = 2500$ Hz at $y = 0.1$ m. Numerical results are obtained with $\alpha = 2.5 \times 10^{-3}$ s^{-1} and the analytical model is performed for $R_r = 0$ and $N = 65$. Comments of these results lead to the same conclusions as for $f = 2000$ Hz: the analytical model predicts with a good accuracy the acoustic field except for the amplitude in the very near field and underestimates the attenuation at the end of the street; the numerical model predicts with a good accuracy the acoustic field only far from the source (from 1 m) only.

Table 1 presents the reflection coefficient R_r and the absorption coefficient α versus frequency. The absorption coefficient increases with the frequency which denotes that the open roof of the street tends to be transparent when the frequency increases. The reflection coefficient magnitude decreases with the frequency increase and reaches zero for highest frequencies. However, it does not mean that there is no reflection of the acoustic waves on the open roof since the attenuation is modeled by a single coefficient R_r depending on the frequency and the street size. Actually, for higher frequencies, each mode has its own reflection coefficient as illustrated by the following section.

5.3. Frequency limit of the model

Fig. 9 shows the map of the experimental acoustic pressure magnitude along the street for $f = 3400$ Hz with a square source centered on ($y_s = 0.1$ m, $z_s = 0.07$ m). On Fig. 10, the acoustic pressure profile at $y = 0.1$ m is represented.

These figures highlight clearly two modal behaviors of the pressure field along the x-axis. At the beginning of the street (until 1 m), the mode defined by $2\lambda = d$ along the y-axis is clearly predominant with an attenuation illustrated by the shaded line on Fig. 10. A second mode, defined by $\lambda/2 = d$, is also visible on Fig. 10 with an attenuation illustrated by the solid line. Because the attenuation of this second mode is weaker than the first one, only this mode remains in the second part of the street (from 1 m).

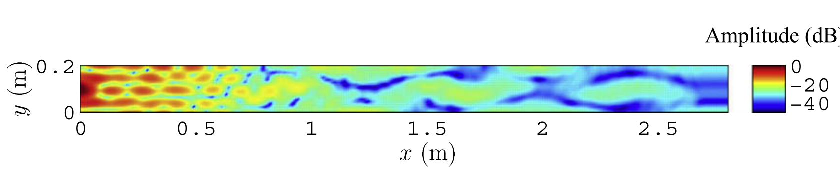

Fig. 9. Experimental acoustic pressure in a street at $z = 0.07$ m, for a frequency $f = 3400$ Hz and for a square source centered on ($y_s = 0.1$ m, $z_s = 0.07$ m).

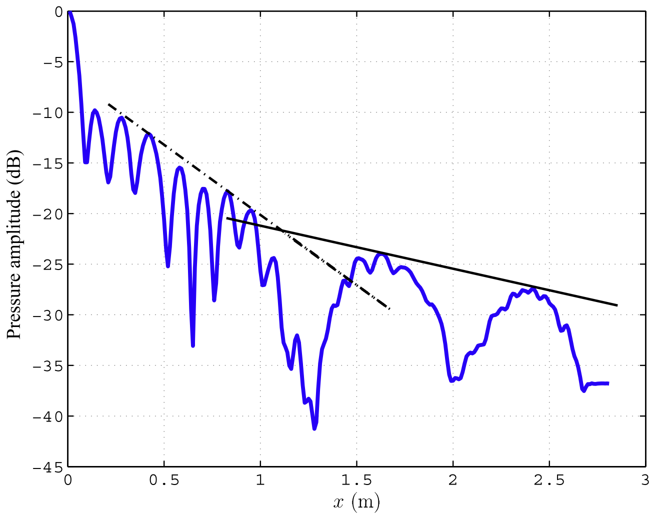

Fig. 10. Experimental pressure profile along the street for $f = 3400$ Hz (see Fig. 9 for geometrical configuration) at $y = 0.1$ m.

The analytical and numerical models, used in this work, cannot describe such a behavior with one single reflection or absorption coefficient. These experimental results show the frequency limit of these models. In order to model attenuation depending on each mode, the notion of leaky modes [22] must be used. In this case, the mode has to be defined by taking into account the losses due to the open roof, so the 2D geometry of the street section and not only the width of the street.

6. Conclusion

This paper deals with the open roof effect on the acoustic propagation in a street at low frequencies. A numerical model, based on an adapted 2D-FDTD simulation describing the open roof effect by means of a single absorption coefficient, shows a good agreement with the experimental data obtained in a street scale model and reveals a losses increase with the frequency. An analytical model, based on modal and image source approaches, describing the open roof effect by means of a reflection coefficient, is developed. Agreement with experimental data is good at low frequencies with a small divergence (far from the source) due to the rigid facade assumption. The reflection due to the open roof decreases and tends to zero when the frequency increases. For higher frequencies, these models are limited by the presence of leaky modes propagating with different attenuation.

Prospects will concern the introduction of the facade absorption in the models and the determination of the reflection coefficient for each mode and their dependence on frequency.

Acknowledgements

The authors thank S. Lebon, E. Egon, P. Collas and P.E. Chartrain for their help on the experimental system, post-processing computation and experimental study.

References

[1] Wiener FM, Malme CI, Gogos CM. Sound propagation in urban areas. J Acoust Soc Am 1965;37:738–47.
[2] Oldham DJ, Radwan MM. Sound propagation in city streets. Build Acoust 1994;1:65–8.
[3] Picaut J, Simon L, Polack J-D. Sound field in long rooms with diffusely reflecting boundaries. Appl Acoust 1999;56:217–40.
[4] Picaut J, Simon L, Polack J-D. Sound propagation in urban areas: a periodic disposition of buildings. Phys Rev E 1999;60:4851–9.
[5] Van Renterghem T, Botteldooren D. Prediction-step staggered-in-time FDTD: an efficient numerical scheme to solve the linearised equations of fluid dynamics in outdoor sound propagation. Appl Acoust 2007;68:201–16.
[6] Albert DG, Liu L, Moran ML. Time reversal processing for sound source location in an urban environment (l). J Acoust Soc Am 2005;118(2):616–9.
[7] Bullen R, Fricke F. Sound propagation in a street. J Sound Vib 1976;46:33–42.
[8] Hornikx M, Forssén J. The 2.5-dimensional equivalent sources method for directly exposed and shielded urban canyons. J Acoust Soc Am 2007;122(5):2532–41.
[9] Hornikx M, Forssén J. Noise abatment shemes for shielded canyons. Appl Acoust 2009;70:267–83.
[10] Wu S, Kittinger E. On the relevance of sound scattering to the prediction of trafic noise in urban streets. Acustica 1995;81:36–42.
[11] Lu KK, Li KM. The propagation of sound in narrow street canyons. J Acoust Soc Am 2002;112:537–50.
[12] Kang J. Sound propagation in street canyons: comparison between diffusely and geometrically reflecting boundaries. J Acoust Soc Am 2000;107:1394–404.
[13] Bradley JS. A study of traffic noise around buildings. Acustica 1977;38:247–52.
[14] Kang J. Numerical modelling of the sound fields in urban streets with diffusely reflecting boundaries. J Sound Vib 2002;258:793–813.
[15] Le Bot A. A functional equation for the specular reflection of rays. J Acoust Soc Am 2002;112:1276–87.
[16] Kang J. Numerical modelling of the sound fields in urban square. J Acoust Soc Am 2005;117(6):3695–706.
[17] Le Pollés T, Picaut J, Bérengier M. Sound field modelling in a street canyon with partially diffusely reflecting boundaries by a transport theory. J Acoust Soc Am 2004;116:2969–83.
[18] Ögren M, Forssén J. Modelling of a city canyon problem in a turbulent atmosphere using an equivalent sources approach. Appl Acoust 2004;65:629–42.
[19] Heimann D. Three-dimensional linearised Euler model simulations of sound propagation in idealised urban situations with wind effects. Appl Acoust 2007;68:217–37.
[20] Picaut J, Simon L. A scale model experiment for the study of sound propagation in urban areas. Appl Acoust 2001;62:327–40.
[21] Redondo J, Pico R, Roig B, Avis MR. Time domain simulation of sound diffusers using finite-difference schemes. Acustica 2007;93(4):611–22.
[22] Pelat A, Felix S, Pagneux V, Ayrault C, Richoux O. Sound propagation in a street canyon: a study by modal decomposition. In: Proceedings of the second ASA–EAA joint conference Acoustics08 Paris, Paris, France; 2008.